Stimulated Emission of Surface Plasmon Polaritons in a Microcylinder Cavity

J. K. Kitur, V. A. Podolskiy, and M. A. Noginov

Stimulated Emission of Surface Plasmon Polaritons in Microcylinder Cavity

M. A. Noginov[1], J. K. Kitur[1], V. A. Podolskiy[2]

[1] Center for Materials Research, Norfolk State University, Norfolk, VA 23504

[2] Department of Physics and Applied Physics, University of Massachusetts Lowell, Lowell, MA 01854

mnoginov@nsu.edu

Abstract

We have observed stimulated emission of surface plasmon polaritons (SPPs) in dye-doped polymeric microcylinder cavities deposited onto gold and silver wires. The stimulated emission spectra featured characteristic series of laser modes, with modal spacing corresponding to SPPs propagating at the interface between metal and dielectric. Plasmonic micro-laser adds to the toolbox of plasmonic devices and plasmonic metamaterials and enables on-chip plasmonic generation and loss compensation.

Most metamaterials – engineered media with rationally designed geometry, composition, and arrangement of nanostructured inclusions – rely on surface plasmons (SPs) to enable sub-diffraction focusing, sub-wavelength resolution imaging, and invisibility cloaking [1-10]. SPs are also widely used in photonic and electronic devices that include waveguides, couplers, splitters, add/drop filters [11-13], light sources [14-16], and sensors [11]. Unfortunately, most applications of SPs at optical frequencies are severely limited by absorption losses. Incorporation of optical gain into adjacent dielectric [17-20] can compensate absorption in metal and, thus, enable long-

awaited applications of metamaterials [1-10]. Moreover, it can open new avenues of light manipulation at subwavelength scale, which include coherent generation of photons and plasmons [15,16,21,22] and logic switching between two states.

Increase of propagation length of surface plasmons (also known as surface plasmon polaritons, SPPs) by creating population inversion and gain in a dielectric medium adjacent to a metallic film was first theoretically proposed in Ref. [17]. Gain-assisted propagation of SPPs in planar metal waveguides of different geometries has been further studied theoretically in Ref. [23]. The partial compensation of SPP loss by gain has been demonstrated in Kretschmann geometry [24] in Ref. [19].

In Ref. [25], stimulated emission of SPPs, manifested by narrowing of SPP emission spectra and characteristic to lasers threshold behavior, has been observed when optical gain in a dye-doped polymeric film deposited on the top of a silver film overcame the SPP loss. The effect described in Ref. [25], was most likely an SPP amplification in open paths. Whether a feedback provided by SPP scattering (similar to that in random lasers [26]) existed in the system, it did not have a distinctive signature in the emission behavior.

In this work, we demonstrate stimulated emission in metal-dielectric ring cavities originating from SPPs propagating at the interfaces between cylindrical gold or silver wires surrounded by dye-doped polymers. The SPPs are excited by optically pumped dye molecules emitting into surface plasmon polariton modes [25,27,28].

Microcylinder cavities were fabricated by dipping gold and silver wires (10 μm and 27.2 μm diameters, respectively) into a dichloromethane solution of polymethyl methacrylate (PMMA) and rhodamine 6G dye (R6G) and drying resulting polymeric films in air. A microcylinder cavity deposited onto a 37 μm diameter glass fiber was used as a reference. Depending on the viscosity

of the solution, the polymer film thickness varied between 1 µm and 10 µm. Thick films (produced from highly viscous solutions) had significant irregularities of their outer surfaces while thin films (deposited using much less viscous solutions) had considerably better quality. The concentration of dye molecules in dry polymer was equal to 10 g/l (2.1×10^{-2} M).

The samples were pumped from the side with ~10 ns pulses of a frequency-doubled Nd:YAG laser (λ=532 nm). The diameter of the pumped spot was equal to ~0.25 mm. The samples' emission was collected (at right angle in respect to the direction of the pumping beam) by a lens and directed to an entrance slit of a monochromator, which had a photomultiplier tube connected to its exit slit.

The thickness of the (reasonably good quality) PMMA/R6G film deposited onto the glass fiber was equal to ~1 µm (outer diameter 39 µm). At weak pumping of this sample (0.34 mJ), only spontaneous emission characterized by the maximum at $\lambda \approx 570$ nm has been observed in the spectrum. With an increase of the pumping energy to 0.53 mJ, a series of sharp spectral lines manifesting an onset of the stimulated emission in cylindrical cavities [29] appeared on the top of a broader spontaneous emission band.

The emission spectrum of the microcylinder laser was mapped on the spectrum of whispering gallery modes, approximated by [29,30]

$$\lambda_m = \frac{\pi n d}{m},$$

where m is the mode number, n is the refractive index and d is the outer diameter of the ring. Correspondingly, the inter-modal separation (measured in units of wavenumbers $\Delta\left(\dfrac{1}{\lambda}\right)$ [cm^{-1}] and proportional to the frequency mode spacing $\Delta\nu$ [s^{-1}]) can be used to determine the product nd,

$$\Delta\left(\frac{1}{\lambda}\right) = \frac{1}{\pi n d} \; .$$

From the dependence of the mode spectral position on the mode number (upper inset of Fig. 1a) we have calculated $\Delta\left(\frac{1}{\lambda}\right)$=55 cm^{-1} and nd=58 µm. Alternatively, the Fourier transform (FT) of the emission spectrum was calculated, revealing a series of equidistant peaks corresponding to multiples of nd [29], see Fig. 1b and inset of Fig. 1b. The product nd determined from the Fourier transform analysis was equal to 56 µm. A good agreement between the latter two values and the one that can be calculated based on the knowledge of the refractive index of R6G-doped PMMA (n=1.5) and the outer diameter of the microcylinder cavity, nd=1.5x39 µm=58.5 µm, proves that the two methods are accurate enough and can be used for analysis of the mode structure of SPP lasers described below.

The microcylinder cavity deposited onto 10 µm diameter gold wire had outer diameter equal to ≈33 µm, see inset of Fig. 2a. Emission spectra recorded at large and small pumping energies in this sample (Fig. 2a) were qualitatively similar to those in Fig. 1a. The analysis of the inter-mode spacing and the Fourier transform (see Figs. 2b and 2c) yielded the product nd to be equal to 19.9 µm and 19.6 µm, respectively.

The refractive index of SPPs propagating at the almost-planar interface between gold and PMMA is equal to $n_{SPP} = \mathrm{Re}\left(\sqrt{(\varepsilon_{PMMA}\varepsilon_{Au})/((\varepsilon_{PMMA}+\varepsilon_{Au}))}\right)$=1.74 at λ=590 nm [24,31], where ε_{PMMA} and ε_{Au} are electric permittivities of PMMA and gold, respectively. The diameter of the wire is approximately equal to 10 µm and the corresponding product $n_{SPP}d$ =17.4 µm is close to that measured experimentally. On the other hand, if existed, the whispering gallery mode concentrated at the outer diameter of ≈33 µm gold-PMMA cylinder would have $n'_{PMMA}d$ =49 µm.

This proves that the observed stimulated emission modes of a ring cavity were due to surface plasmon polaritons propagating at the surface of the gold wire.

The outer diameter of the microcylinder cavity deposited onto 27.7 μm diameter silver wire was equal to 39.3 μm. The series of emission spectra taken at different pumping energies is shown in Fig. 3. The product nd calculated from the direct measurement of the inter-mode spacing was equal to 40.2 μm and that obtained from the Fourier analysis was equal to 41.1 μm. The refractive index of SPPs propagating at interface between silver and PMMA is equal to n =1.62 at λ=590 nm [31], corresponding to the product nd=43.5 μm, which is close to that measured experimentally. On the other hand, the whispering gallery mode residing at the outer diameter of the 39.3 μm PMMA cylinder would have nd =59 μm. The difference between this value and the experimentally measured ones exceeds the experimental error (≤10%). We thus conclude that the stimulated emission in a microcylinder cavity on a silver wire originated from the SPP modes as well. Note that the shift of the stimulated emission range to shorter wavelengths with the increase of the pumping (traces 2 and 3 of Fig. 3) is typical of dye lasers. The wavelength of the stimulated emission is determined by a trade-off of absorption and gain. At low pumping the lasing starts at longer wavelength. As pumping increases, the laser wavelength moves closer to the maximum of the gain band and, correspondingly, to shorter wavelengths.

To further analyze the behavior of the SPP waves on the cylinder, the spectrum of the modes, their lifetimes, and lasing frequencies were simulated using S-matrix formalism [30], where the field in each cylindrical segment of the system was represented as a set of cylindrical waves, and emission properties of the resonator were defined by the singularity of reflectivity determined by scattering (S) matrix that relates the amplitudes of these waves. In the set of simulations, we

5

considered SPP propagating at the gold wire-PMMA interface. The modal spacing determined from these simulations (Fig. 4) was consistent with the one obtained in the experiment (Fig. 2). Our simulations also confirm that the lifetime of the SPP mode is comparable to the lifetime of the SPP propagating at the planar metal-dielectric interface, so that the decay rate corresponding to diffraction-induced leaking of the mode from the curved surface is relatively small.

As mentioned above, the shapes of outside walls of microcylinder resonators deposited onto metallic wires deviated from perfect cylinders, with boundary roughness exceeding 2μm. (In the gold wire, inhomogeneities (caverns) in the outer cylinder wall were ≥ 2 μm-deep and ~5 μm-large in longitudinal and azimuthal dimensions. In the silver wire, radial deviations from an ideal cylinder were even larger, ≥ 4 μm in all dimensions.) Polymeric films deposited onto glass fibers had much better surface quality, but also were not free of imperfections. As shown in [30,32], deformation of resonator boundary drastically reduces quality factors of photonic modes that rely on repeated total internal reflection from external resonator boundary by destroying the stability of quasi-periodic whispering gallery modes and introducing a chaos-assisted tunneling process [32]. This explains why the stimulated emission supported by purely photonic whispering gallery modes was not observed in microcylinder cavities deposited onto gold and silver wires and had relatively high thresholds in the films deposited on the glass fibers. In contrast, SPPs were highly confined to the proximity of a much smoother metal-dielectric interface. As result, the stimulated emission thresholds of SPP modes were comparable to or even lower than those of perturbed whispering gallery modes in polymeric films on glass fibers.

The available pumping density in our experiments was nearly two orders of magnitude higher than the saturation pumping density of R6G, guaranteeing that nearly all dye molecules were excited. A ballpark estimate shows that the resulting gain in the system was of the same

order of magnitude as required to compensate the absorption loss of SPPs. This further supports our conclusion that the observed stimulated emission in both gold and silver-based microcylinder cavities originated from SPPs propagating at the interface between metal and dielectric.

To summarize, we have observed lasing in microcylinder cavities formed by dye-doped polymer deposited on gold and silver wires. The analysis of the mode structure proves that the stimulated emission originates from surface plasmon polaritons propagating at the interface between metal and dielectric. We would like to emphasize that the demonstrated device generated coherent propagating surface plasmon polaritons rather than photons, which were produced in a secondary process *via* outcoupling of SPPs to vacuum modes. This made it conceptually similar to a spaser that was originally proposed to generate coherent localized surface plasmons in a metallic nanostructure surrounded by gain medium [21].

Note that the combination of the polymer and the solvent used in our experiments (the same as was employed in our previous studies of SPPs and gain [25]) was not optimal for precise control of the film thickness and quality, which affected the reproducibility of thick-film samples. (The films' properties above strongly depend on the viscosity of the polymer-dye solution – the parameter highly sensitive to the solvent temperature, its evaporation rate, etc.) The literature [33-35] suggests that a more favorable combination of a polymer and a solvent can be found. Results of these studies are to be published elsewhere.

The demonstrated micro-lasers extend the family of practical plasmonic devices by adding to it an active stimulated emission tool, which can also operate as an amplifier. Coupling plasmonic microlasers to plasmonic waveguides will allow one to deliver generated and amplified SPs to integrated plasmonic and electronic circuits on demand, enabling dream applications of information technology operating at optical frequencies.

References

1. V.G. Veselago, Sov. Phys. Uspekhi **10**, 509-514 (1968).

2. J.B. Pendry, Phys. Rev. Lett **85**, 3966 (2000).

3. A. Grbic and G. Eleftheriades, Phys. Rev. Lett **92**, 117403 (2004).

4. N. Fang, H. Lee, C. Sun, and X. Zhang, Science **308**, 534 (2005).

5. I.I. Smolyaninov, Y.J. Hung, and C.C. Davis, Science 315, 1699 (2007).

6. Z. Jacob, L. V. Alekseyev, and E. Narimanov, Opt. Express 14, 8247-8256 (2006).

7. A. Salandrino and N . Engheta, Phys. Rev *B* **74**, 075103 (2006).

8. U. Leonhardt, Science **312**, 1777-1780 (2006).

9. J.B. Pendry, D. Schurig, and D.R. Smith, Science **312**, 1780 (2006).

10. W. Cai, U.K. Chettiar, A.V. Kildishev, and V.M. Shalaev, Nature Photonics **1**, 224 (2007).

11. S.I. Bozhevolnyi, Pan Stanford Publishing: Singapore, (2008).

12. Maier, S.A. et al. Local detection of electromagnetic energy transport below the diffraction limit in metal nanoparticle plasmon waveguides. *Nature Materials* **2**, 229-232 (2003).

13. Stockman, M. Nanofocusing of optical energy in tapered plasmonic waveguides. *Phys. Rev. Lett* **93**, 137404 (2004).

14. C. Sirtori *et al.,* Opt. Lett **23**, 1366-1368 (1998).

15. M.T. Hill *et al.*, Opt. Express **17**, 11107-11112 (2009).

16. R.F. Oulton *et al.*, Nature **461**, 629-632 (2009).

17. A.N. Sudarkin and P.A. Demkovich, Sov. Phys. Tech. Phys **34**, 764-766 (1989).

18. N.M. Lawandy, Appl. Phys. Lett **85**, 5040-5042 (2004).

19. J. Seidel, S. Grafstroem, and L. Eng, Phys. Rev. Lett **94**, 177401 (2005).

20. M.A. Noginov *et al.*, Opt. Lett **31**, 3022-3024 (2006).

21. D. Bergman and M. Stockman, Phys. Rev. Lett **90**, 027402 (2003).

22. M.A. Noginov *et al*., Nature **460**, 1110-1112 (2009).

23. M.P. Nezhad, K. Tetz, and Y. Fainman, Opt. Express **12**, 4072-4079 (2004).

24. H. Raether, *Surface plasmons on smooth and rough surfaces and on gratings* (Springer-Verlag, Berlin, 1988).

25. M.A. Noginov *et al*., Phys. Rev. Lett **101**, 226806 (2008).

26. M.A. Noginov, *Solid-state random lasers* (Springer, New York, 2005).

27. W. H. Weber, C. F. Eagen, Opt. Lett. 4, 236-238 (1979).

28. Krishanu Ray, et al., Appl. Phys. Lett., **90**, 251116/1-3 (2007).

29. R. C. Polson, Z. V. Vardeny, and G. Levina, Synthetic metals **116**, 363-367 (2001).

30. O. A. Starykh, P. R. J. Jacquod, E. E. Narimanov, and A. D. Stone, Phys. Rev. *E* **62**, 2078 (2000).

31. P. B. Johnson and R. W. Christy, Phys. Rev *B* **6**:4370-4379 (1972).

32. V. A. Podolskiy and E. E. Narimanov, Opt. Lett **30**, 474 (2005).

33. H. R. Allcock, F. W. Lampe, J. E. Mark, Contemporary polymer chemistry, Third Edition, Pearson Prentice Hall, Upper Saddle River, New Jersey (2003) 814 p.

34. J. Brabdrup, E. H. Immergut, E. A. Grulke, Polymer handbook, Fourth edition, Wiley (2003) 2336 p.

35. J. E. Mark, Physical properties of polymers handbook, Springer, (2006).

Figure Captions

Fig. 1. (a) Emission spectra of a microcylinder PMMA/R6G laser on a glass fiber: trace 1 – 0.34 mJ, spontaneous emission; trace 2 – 0.53 mJ, stimulated emission. Upper inset: Dependence of the mode energy *vs* mode number (counted starting from the first mode which can be seen in the spectrum). Lower inset: Schematic of a PMMA/R6G microcylinder cavity on a fiber or wire. (b) Fourier transform of the emission spectrum in Fig. 1a (0.53 mJ) plotted against *nd*. Inset: Position of the FT peak (in units of *nd*) *vs* FT peak number.

Fig. 2. (a) Emission spectrum of R6G/PMMA-coated gold wire; trace 1 – 0.026 mJ, trace 2 – 0.052 mJ. Inset: microphotograph of the wire; top part – 10 μm bare gold wire, bottom part – ~30 μm wire coated with R6G/PMMA. (b) Dependence of the mode energy *vs* mode number (c) Position of the FT peak (in units of *nd*) *vs* FT peak number.

Fig. 3. Emission spectrum of R6G/PMMA-coated silver wire; trace 1 – 0.085 mJ, trace 2 – 0.175 mJ, trace 3 – 0.228 mJ. Lower inset: Dependence of the mode energy *vs* mode number. Upper inset: Position of the FT peak (in units of *nd*) *vs* FT peak number.
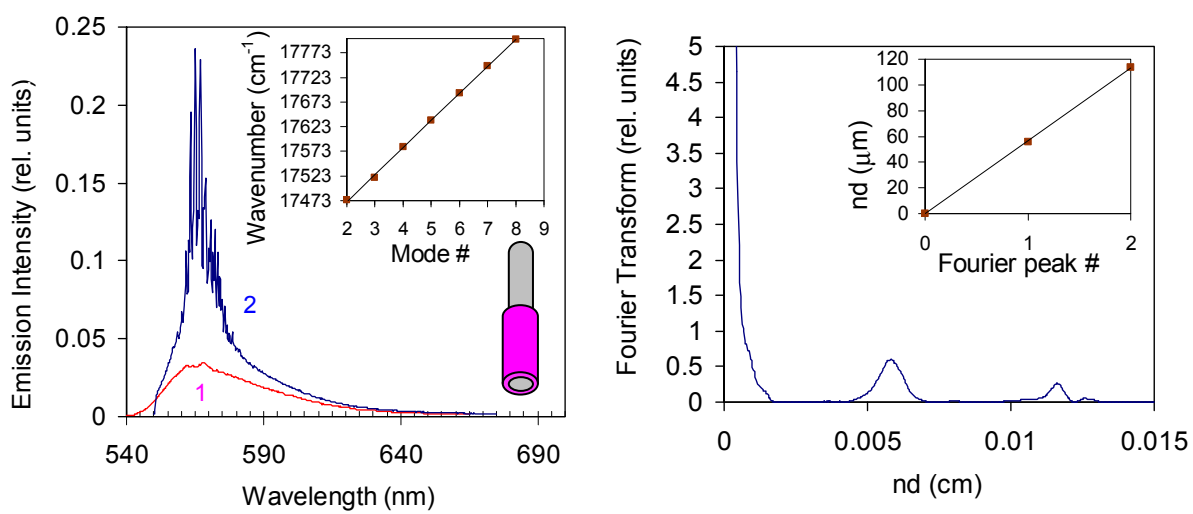
Fig. 4. Eigen-frequencies of Au-PMMA microcylinder resonator.
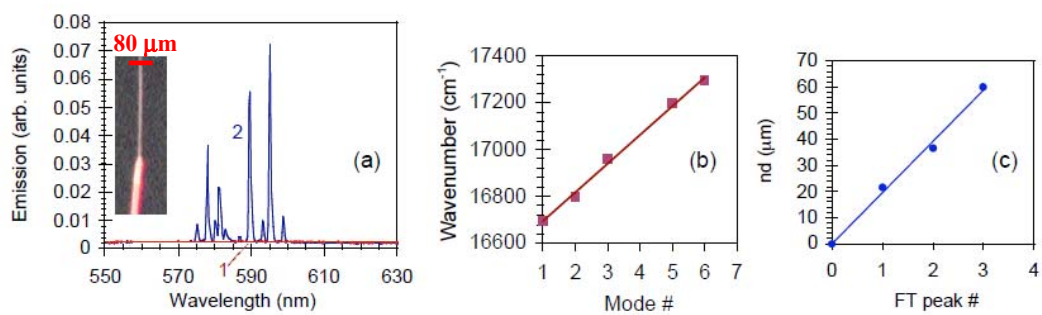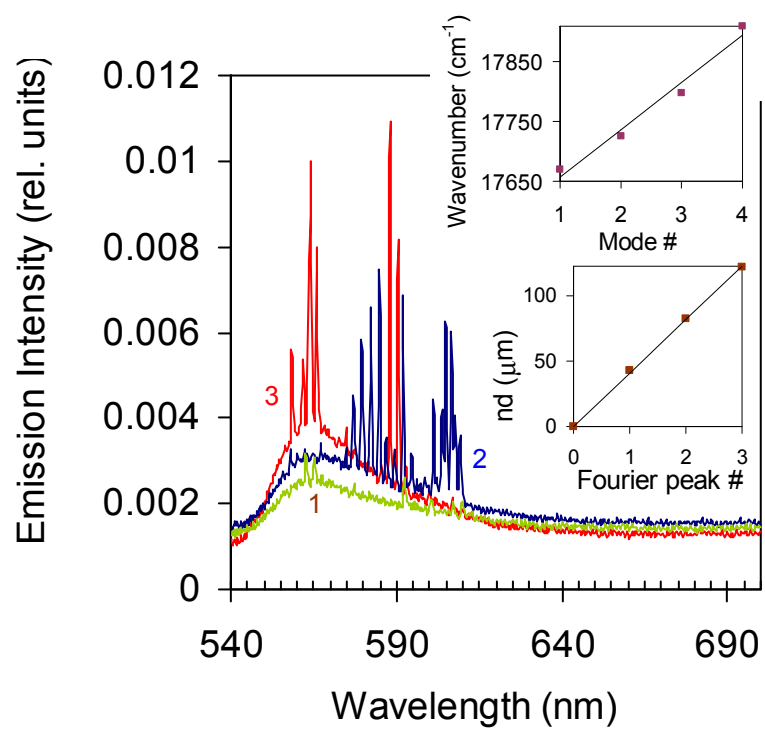
Figure 1.

Figure 2.

Figure 3.

Figure 4.